

Ab initio molecular dynamics for liquid metals

G. Kresse and J. Hafner

Institut für Theoretische Physik, Technische Universität Wien, Wiedner Hauptstrasse 8-10, A-1040 Wien, Austria

(Received 8 July 1992; revised manuscript received 9 October 1992)

We present *ab initio* quantum-mechanical molecular-dynamics calculations based on the calculation of the electronic ground state and of the Hellmann-Feynman forces in the local-density approximation at each molecular-dynamics step. This is possible using conjugate-gradient techniques for energy minimization, and predicting the wave functions for new ionic positions using sub-space alignment. This approach avoids the instabilities inherent in quantum-mechanical molecular-dynamics calculations for metals based on the use of a fictitious Newtonian dynamics for the electronic degrees of freedom. This method gives perfect control of the adiabaticity and allows us to perform simulations over several picoseconds.

A few years ago Car and Parrinello¹ introduced an approach that unifies molecular-dynamics techniques for the calculation of the atomic structure with the local-density approximation² (LDA) for electronic structure calculations, with the complete set of quantum-mechanical many-body forces calculated using the Hellmann-Feynman theorem. The basic idea is the introduction of a fictitious dynamics for the electronic degrees of freedom. Since the electronic wave functions of the LDA are meaningful only if the electrons are in their ground state for the instantaneous ionic configuration, an essential condition for the practicability of the Car-Parrinello method is that the transfer of energy between the atomic and electronic subsystems is small in order to prevent the electron states to drift away from the ground states. This transfer of energy is difficult to control in metallic systems. In insulators, the width of the electronic band gap divided by the fictitious mass of the electronic degrees of freedom defines the separation in the characteristic frequencies of the atomic and electronic motions. In metals, this separation is absent and there are essentially two mechanisms that drive metallic systems into nonadiabaticity: a resonance between the atomic and electronic frequencies opening a channel for energy transfer and a level crossing between occupied and empty electron states.³ The operational solution of these nonadiabaticity problems is (a) to perform periodic energy minimizations⁴ to bring the system "back to the Born-Oppenheimer surface" or (b) to attach the electronic subsystem to a Nosé thermostat that prevents the heating up of the electron system.⁵ Clearly the alternative is to perform the minimization of the Kohn-Sham functional for the electronic total energy at any time step of the molecular-dynamics simulation, so that the problem of the nonadiabaticity does not arise at all. An efficient way to perform the minimization process are conjugate-gradient methods.⁶⁻⁸ These techniques have now been developed to a point where it is possible to perform canonical molecular-dynamics simulations for liquid metals over periods of several picoseconds, with complete control over deviations from adiabaticity and good energy conservation. Applications for liquid metals ranging

from Na to Ge demonstrate very good agreement with the measured atomic structure factors and electronic spectra.

Our technique for performing a complete calculation of the LDA ground state after each molecular-dynamics step is based on the conjugate-gradient techniques developed by Payne and co-workers.⁶⁻⁸ and used in self-consistent electronic structure calculations by Bylander, Kleinman, and Lee.^{9,10} The method is a doubly iterative one: in the inner loop the wave functions for each \mathbf{k} point in the Brillouin zone and each band are improved by a preconditioned conjugate-gradient method as described in Ref. 9 until the change in the energy eigenvalue is smaller than 10^{-6} eV (or smaller than 30% of the change in the first step). After running over all bands (including some empty bands), a subspace diagonalization is performed, the new Fermi energy is calculated using a Gaussian broadening of the energy levels, and the charge density is updated. The problems arising from using fractional occupation numbers and their consequences for *ab initio* molecular-dynamics simulations have been discussed by Weinert and Davenport¹¹ and by Wentzcovitch, Martins, and Allen.¹² It has been shown that the variational quantity is not the internal energy but a generalized free energy. To prevent charge sloshing, the mixing scheme proposed by Kerker¹³ is used. This scheme has the advantage of damping the oscillations in the low- q components of the charge density. The electronic-energy minimization is terminated when the change in the energy per atom becomes smaller than 1.5×10^{-5} eV.

The atomic motion is described by Nosé dynamics¹⁴ generating a canonical ensemble at prefixed temperature. The equations of motion are integrated using a fourth-order predictor-corrector algorithm^{15,16} which allows the use of time steps as large as 3×10^{-15} s with good energy conservation. After moving the atoms, the new wave functions are estimated by using the subspace alignment proposed by Arias, Payne, and Joannopoulos.⁸

The calculation has been performed for a nonlocal pseudopotential in Kleinman-Bylander factorization, using the real-space projection scheme of King-Smith, Payne, and Lin.⁷

The first test was performed for a 54-atom ensemble

representing liquid Na at $T = 400$ K and a number density of $n = 0.02436 \text{ \AA}^{-3}$. A Vanderbilt pseudopotential¹⁷ with a cutoff radius of $r_c = 2.0$ a.u. has been used. The simulation is started for a configuration of the liquid generated using classical molecular dynamics based on pair forces calculated by pseudopotential perturbation theory from the same pseudopotential. The starting wave functions for this configuration are generated by diagonalizing the Hamiltonian in a basis of 200 plane waves. For the *ab initio* molecular dynamics (MD) the Kohn-Sham orbitals at the Γ -point are expanded into plane waves with a maximum kinetic energy cutoff of 6 Ry, the time step for the integration of the atomic equations of motion being $\Delta t = 3 \times 10^{-15}$ s. For Na the prediction of the wave function by subspace alignment leads to a state whose energy does not differ from the ground-state energy by more than 3×10^{-5} eV/atom. Under those conditions the total energy per ion remains constant within 1

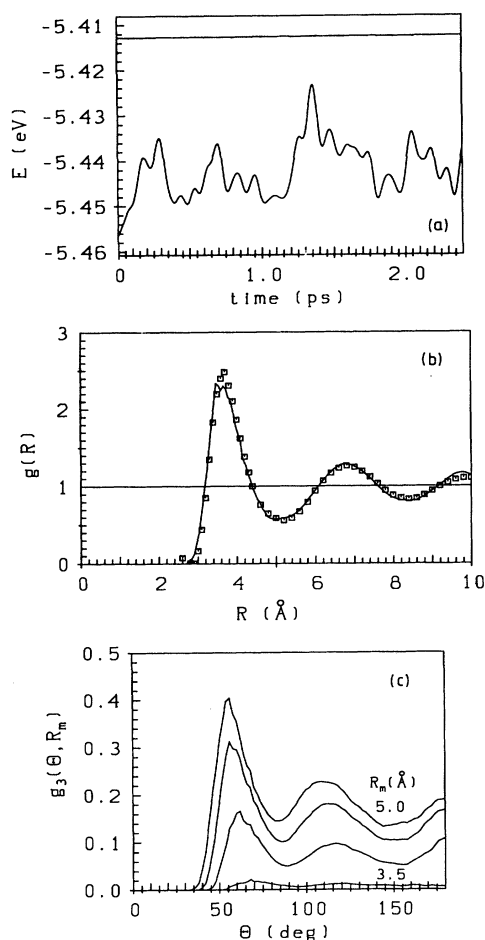


FIG. 1. (a) Variation of the total energy (upper curve) and of the potential energy (lower curve) of liquid Na at $T = 400$ K along an *ab initio* MD run of 2 ps. (b) Pair correlation function for liquid Na at $T = 400$ K; full curve—*ab initio* MD, squares—experiment (Ref. 18). (c) Bond-angle distribution function $g_3(\theta, R_m)$, calculated for different values of the maximum bond length: $R_m = 3.5, 4.0, 4.5,$ and 5.0 \AA .

meV for a run over 2.5 ps [Fig. 1(a)]. Ensemble averages are calculated from the last 1.5 ps of the run. The pair correlation function [Fig. 1(b)] is in excellent agreement with experiment.¹⁸ The coordination number of $N_c = 13$ (obtained by integrating the radial distribution function $4\pi R^2 g(R)$ up to the first minimum) corresponds to an atomic arrangement similar to a dense random sphere packing. Integration over the symmetric part of the first peak leads to a lower value for the coordination number $N_c = 10$. The diffusion constant (calculated by averaging over a number of different starting configurations, for details see Ref. 10) is approximately $D = 6 \times 10^{-5} \text{ cm}^2/\text{s}$, again in reasonable agreement with experiment ($D = 5.3 \times 10^{-5} \text{ cm}^2/\text{s}$; Ref. 19).

A more critical test than the free-electron metal Na is the “bad metal” liquid Ge. We use again a nonlocal Vanderbilt pseudopotential with $r_c = 1.5$ a.u. and Kleinman-Bylander factorization for *s* and *d* nonlocality. With this pseudopotential, we calculate the lattice constant of α -Ge at $T = 0$ K with the diamond structure within 1.3% of the experimental value and a reasonable pressure for the $\alpha \rightarrow \beta$ transition ($P_c = 75$ kbar, expt. $P_c = 100$ kbar), see Fig. 2. For the *ab initio* molecular-dynamics calculations, the wave functions at the Γ point are expanded in a basis of 7000 plane waves with a cutoff energy of 12 Ry. For the real- and reciprocal-space representation of the potential and the charge density a $32 \times 32 \times 32$ mesh is used. For the 64-atom ensemble, we calculated the wave functions for 138 bands, i.e., 10 bands more than necessary to accommodate the 256 valence electrons. A Gaussian broadening width of 0.2 eV was used. Again the simulation was started for a configuration generated by classical molecular-dynamics run. The temperature is $T = 1250$ K, the number density is $n = 0.04385 \text{ \AA}^{-3}$. The prediction of the wave function leads to a state whose energy does not differ from the ground-state energy by more than 5×10^{-5} eV/atom. The change in the total energy per atom (Fig. 3) was 4 meV over a run of 2.7

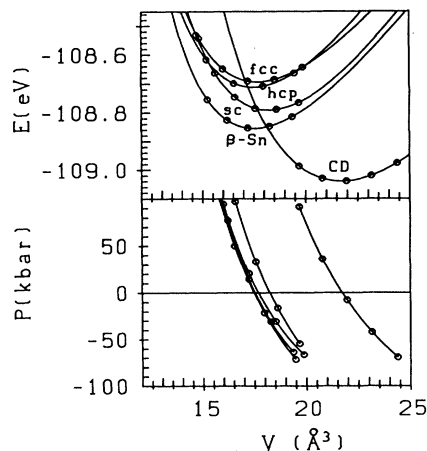


FIG. 2. Energy E and pressure P vs volume V for solid Ge in different crystal structures, calculated with the pseudopotential used in the *ab initio* MD simulation: cubic diamond (CD), β -Sn, face-centered cubic (fcc), hexagonal close-packed (hcp), and simple cubic (sc).

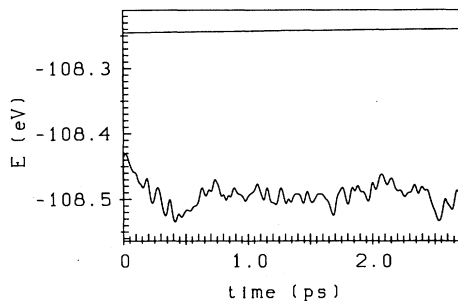


FIG. 3. Variation of the free-energy (upper curve) and of the potential energy (lower curve) of liquid Ge at $T = 1250$ K along an *ab initio* MD run of 2.7 ps.

ps (i.e., 900 steps with $\Delta t = 3 \times 10^{-15}$ s); this is less than 0.1% of the cohesive energy, and corresponds to a temperature of 50 K. The kinetic energy is stabilized by the Nosé thermostat.

The detailed analysis of the atomic structure shows that the atomic arrangement in liquid Ge is very different from that in normal liquid metals. The coordination number, obtained by integrating the radial distribution function up to the first minimum at $R_m = 3.35$ Å is $N_c \approx 6.2$, i.e., considerably lower than the value $N_c \approx 10 - 12$ characteristic for normal metals, but in good agreement with experiment ($N_c = 6.8$; Ref. 18). Besides the first peak, there are only weak local maxima in the pair correlation function $g(R)$ whose experimental position and amplitude are well reproduced by the *ab initio* simulation (Fig. 4). Additional information on the short-range order can be obtained from higher-order correlation functions, in particular the triplet correlation function. Triplet correlations are conventionally expressed in terms of the bond angles between two bonds around a central atom with a maximum bond length R_m . This means that the bond-angle distribution function $g_3(\theta, R_m)$ is just the radial integral over the triplet correlation function $g_3(\theta, R_1, R_2)$ for $R_1 < R_m$ and $R_2 < R_m$. R_m is restricted to distances smaller than the position of the first minimum in $g(R)$. Figure 5 shows that short bonds ($R_m \leq 2.80$ Å) form angles broadly distributed around the tetrahedral angle ($\theta \approx 109^\circ$), whereas longer bonds form angles distributed around $\theta \approx 109^\circ$ and $\theta \approx 60^\circ$.

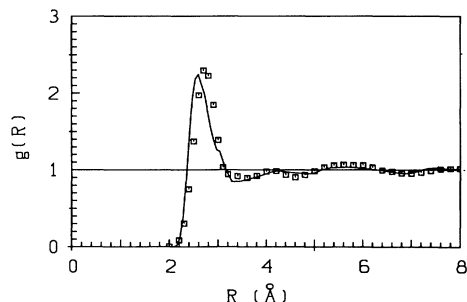


FIG. 4. Pair correlation function $g(R)$ for liquid Ge at $T = 1250$ K: full curve—*ab initio* MD, squares — experiment (Ref. 18).

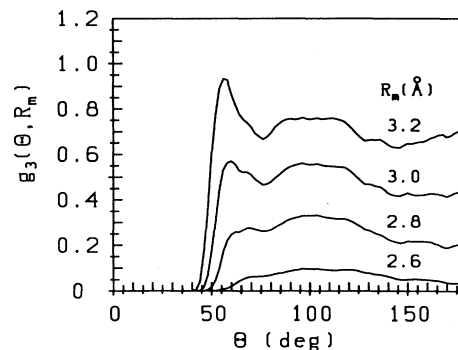


FIG. 5. Bond-angle distribution function $g_3(\theta, R_m)$ for liquid Ge at $T = 1250$ K calculated for different values of the maximum bond length R_m .

The bond-angle distribution $g_3(\theta, R_m)$ in liquid Ge is very different from that in liquid Na [Fig. 1(c)] with pronounced peaks close to the icosahedral bond angles of $\theta = 63.5^\circ$ and $\theta = 116.5^\circ$.

The pair correlations in liquid Ge are reasonably well described on the basis of pseudopotential-derived volume and pair forces.^{16,23,20} We find that differences exist at the level of triplet correlations and in the fluctuations of the local atomic arrangements. These local fluctuations become important at lower temperatures where the system approaches the liquid metal–amorphous semiconductor transition (details will be described elsewhere). The good agreement between the classical and the quantum-mechanical simulations is also important from a computational point of view: it allows one to restrict the time-consuming Hellmann-Feynman-type simulation to states close to the equilibrium and to approach equilibrium in the classical mode. The construction of pseudopotentials that are useful in both aspects has been discussed very recently by Kresse, Hafner, and Needs.²⁰

The electronic density of states (DOS) of liquid Ge obtained by a Gaussian broadening (width 0.4 eV) of the 8×150 lowest eigenvalues at the star of the special k point (0.25, 0.25, 0.25) and averaged over ten configurations is shown in Fig. 6. The characteristic feature is the deep pseudogap about 5 eV below the Fermi level, which is independent of the k space sampling (cf. Refs. 21 and 23). It is interesting that the calculated

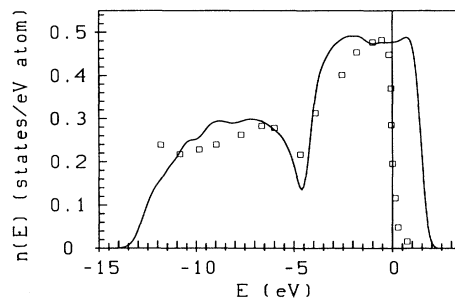


FIG. 6. Electronic density of states $n(E)$ for liquid Ge at $T = 1250$ K: full curve—*ab initio* MD simulation, squares — measured photoemission intensity (Ref. 22).

DOS of liquid Ge is very different from that of any of the crystalline phases: it has neither the characteristic signature of the sp^3 hybridization dominating the DOS of the semiconducting α and the metallic β phases, nor the free-electron-like character of the metallic simple-hexagonal high-pressure phase.²¹ The calculated DOS is in very good agreement with the measured photoemission intensities²² (the experimental resolution is about 0.2 eV) and earlier supercell-linear-muffin-tin-orbital calculations for models of liquid Ge.^{23,21} The breakdown of the sp^3 hybridization is a consequence of the profound change of the atomic short-range order. On melting the coordination number increases from $N_c = 4$ to $N_c \approx 6.5$, and the angular correlation characteristics for tetrahedral bonding are reduced significantly. The pseudogap in the electronic DOS is characteristic for the heavier liquid group-IV elements (Ge, Sn, Pb), but not for *l*-Si, which is much more free-electron-like. It has been shown²³ that the formation of the pseudogap is due to an increasing *s-p* splitting arising from relativistic effects. In Ge it is enhanced by a partial penetration of the 4s electrons into the 3d core, leading to a stronger electron-ion interaction.

We have shown that on the basis of improved conjugate-gradient techniques and the extrapolation of wave functions using subspace-alignment *ab initio* molecular dynamics for liquid metals are feasible without the introduction of a fictitious pseudo-Newtonian dynamics of the electrons. The calculation of the exact Hellmann-Feynman forces at each time step and the use of an accurate predictor-corrector algorithm for the ionic equations of motion allow the use of time steps ($\Delta t \approx 3 \times 10^{-15}$ s) which are of the same order as those used in classical molecular-dynamics routines. This permits one to perform MD runs over several picoseconds. A run of 2.5 ps for liquid Na took less than 12 h CPU time on a Fujitsu-VP 50, a 2.7 ps run for liquid Ge 110 h CPU time. However, to further improve the energy conservation and to extend the length of the simulation remains a challenge.

Our work has been supported by Siemens Nixdorf Austria within the contract of cooperation with the Technische Universität Wien. The support of Dr. M. C. Payne in the early stage of this work is gratefully acknowledged.

¹R. Car and M. Parrinello, Phys. Rev. Lett. **55**, 2471 (1985).

²W. Kohn and L.J. Sham, Phys. Rev. A **140**, 1133 (1965).

³G. Pastore, E. Smargiassi, and F. Buda, Phys. Rev. A **44**, 6334 (1991).

⁴I. Stich, R. Car, and M. Parrinello, Phys. Rev. B **44**, 4262 (1991).

⁵P.E. Blöchl and M. Parrinello, Phys. Rev. B **45**, 9413 (1992).

⁶M.P. Teter, M.C. Payne, and D.C. Allan, Phys. Rev. B **40**, 12255 (1989).

⁷R.D. King-Smith, M.C. Payne, and J.S. Lin, Phys. Rev. B **44**, 13063 (1991).

⁸T.A. Arias, M.C. Payne, and J.D. Joannopoulos, Phys. Rev. B **45**, 1538 (1992).

⁹D.M. Bylander, L. Kleinman, and S. Lee, Phys. Rev. B **42**, 1394 (1990).

¹⁰D.M. Bylander and L. Kleinman, Phys. Rev. B **45**, 9663 (1992).

¹¹M. Weinert and J.W. Davenport, Phys. Rev. B **45**, 13709 (1992).

¹²R.M. Wentzcovitch, J.L. Martins, and P.B. Allen, Phys.

Rev. B **45**, 11372 (1992).

¹³G.P. Kerker, Phys. Rev. B **23**, 3082 (1981).

¹⁴S. Nosé, J. Chem. Phys. **81**, 511 (1984).

¹⁵C.W. Gear, *Numerical Initial Value Problem in Ordinary Differential Equations* (Prentice-Hall, Englewood Cliffs, NJ, 1971), Chaps. 9 and 10.

¹⁶A. Arnold, N. Mauser, and J. Hafner, J. Phys. Condens. Matter **1**, 965 (1989).

¹⁷D. Vanderbilt, Phys. Rev. B **32**, 8412 (1985).

¹⁸Y. Waseda, *The Structure of Non-Crystalline Materials—Liquids and Amorphous Solids* (McGraw-Hill, New York, 1981).

¹⁹S.J. Larsson, C. Roxbergh, and A. Lodding, Phys. Chem. Liq. **3**, 137 (1972).

²⁰G. Kresse, J. Hafner, and R.J. Needs, J. Phys. Condens. Matter **4**, 7451 (1992).

²¹W. Jank and J. Hafner, Europhys. Lett. **7**, 623 (1988).

²²G. Indlekofer, P. Oelhafen, R. Lapka, and H.J. Güntherodt, Z. Phys. Chem **157**, 465 (1988).

²³W. Jank and J. Hafner, Phys. Rev. B **41**, 1497 (1990).